ACCURATE EXTRACTION OF WATER NETWORK ELEMENTS AND THEIR SPATIOTEMPORAL EVOLUTION USING AN IMPROVED DEEPLABV3$^+$ MODEL: A CASE STUDY OF THE ERHAI LAKE BASIN, CHINA

ZHANG, Y.[1] – ZENG, W. J.[1,2,3] – ZHAO, H.[4] – WU, X. C.[1] – HUANG, Y. N.[1] – CHEN, Y. C.[1,2,3] – GUO, X. F.[1,2,3] – ZHANG, J. S.[1*]

[1]*College of Water Resources and Hydraulic Engineering, Yunnan Agricultural University, Kunming 650201, China*

[2]*Yunnan International Joint R&D Center of Smart Agriculture and Water Security, Kunming 650201, China*

[3]*Green Smart Agricultural Field and Carbon Emission Reduction Engineering Research Center of University in Yunnan Province, Kunming 650201, China*

[4]*College of Resources and Environment, Yunnan Agricultural University, Kunming 650201, China*

[*]*Corresponding author*
e-mail: woaishuibao@163.com

(Received 21st Sep 2025; accepted 23rd Dec 2025)

Abstract. The water network (WN) not only plays a part in our daily life, but also partly determines the regional planting structure and ecological pattern. Therefore, using Jilin-1 Gaofen satellite imagery (0.75 m), this study innovatively proposed an improved DeepLabV3$^+$ deep-learning semantic segmentation model to extract WN elements (nodes, arcs, and polygons) in three typical sub-basins of the Erhai Lake Basin, China, for the years 2001, 2008, 2015 and 2023, thereby unveiling the spatiotemporal evolutionary patterns and trends of the WN in the basin. It was found that 1) our improved DeepLabV3$^+$ model could effectively extract complex WN elements, reaching a precision of 98.87%; specifically, it showed robust performance in extracting small objects, effectively suppressed noises from building shades, vegetation occlusions, and complex ground objects; 2) the Northern Three-River Sub-basin it demonstrated the most drastic changes and increasing WN connectivity; in the Cangshan Mountain Sub-basin, the WN experienced less intense variations, and the WN elements grew increasingly independent from each other; WN elements in the Southern Boluo River Sub-basin showed milder variations and declined WN connectivity; 3）as of 2023, the density of WN in the Northern Three-River Sub-basin and Cangshan Mountain Sub-basin has increased, with Sanying Town (19.37) and Xizhou Town (15.70) marking the highest densities, respectively, while the Southern Polo River Sub-basin showed a decreasing density, with Fengyi Town (34.71) having the highest density.
Keywords: *deep learning semantic segmentation, remote sensing, Jilin-1 Gaofen satellite imagery, spatiotemporal evolution*

Introduction

The spatiotemporal distribution of WN elements not only affects the regional life and production, but also has significant impacts on land use, planting structure, and ecological patterns (Wang et al., 2023; Tang et al., 2025). Variations in land use and planting structures and resources, along with terrestrial pollutant transport, thereby affect the health of regional ecosystems (Xu et al., 2021). Therefore, unveiling the spatiotemporal

http://www.aloki.hu ● ISSN 1589 1623 (Print) ● ISSN1785 0037 (Online)
DOI: http://dx.doi.org/10.15666/aeer/2401_15391561

distribution pattern and trend of WN elements is crucial for the protection of regional ecosystems.

Existing studies on water networks focus on the connectivity within the water network (Yan et al., 2008), distribution pattern (Yang et al., 2016), the spatial and temporal distribution (Lu et al., 2023). Precise extraction of water network systems, the basis for structural analysis of the water network and a hot topic in remote sensing data processing (Kumar et al., 2021), can now rely on mature techniques and methods. Through extraction and analysis of features, such as the connection between the dots, lines, and planes in the water network, the density, centrality, and edges of the water network, structural optimization of the network can be performed (Abed-Elmdoust et al., 2016). The fractal dimension, which measures the irregularity of a water network system, is a key indicator of the distribution feature of the network (Wang et al., 2020). To sum up, there have been plenty of works that explored feature extraction and fractal analysis of water networks, with natural water networks as the main research object and the Invest model as the research method. However, a comparative assessment of basin-scale spatial heterogeneity is lacking, and the linkage roles of nodes with polygonal waterbody elements—such as reservoirs, ponds, and wetlands—within the WN remain unclear.

The No. 1 Central Document that China issued in 2023 pinpointed the need to accelerate large water conservancy projects and develop the pillar water networks in the nation (Zhao et al., 2023a), indicating that protection of key water networks has risen to be one of the nation’s priorities. Erhai Lake, an alpine fault semi-closed lake, suffers ecological vulnerability because of its unique terrain, topology, and complex system of water systems (Lin et al., 2020). Since the local government started to speed up adjustments to the land planting structure in the basin in 2015 in its attempt to protect Erhai Lake, many areas of farmland shifted to land for non-agricultural purposes, the area of land for crops requiring higher supplies of water and fertilizers reduced, the utilization efficiency of farmland water decreased, and direct of discharge of water to rivers soared. Changes like these tipped the previous balance of water resources in the basin and resulted in drastic spatial and temporal variations in the basin (Feng et al., 2024). Moreover, the spatiotemporal distribution patterns and developmental trends of WN evolution in the Erhai Lake Basin remain unclear.

To address the challenges mentioned above, this study tried to employ the deep learning semantic segmentation of water bodies in high-resolution remote-sensing imagery, and proposed an improved DeepLabV3$^+$ model. With the original DeepLabV3$^+$ as the overall segmentation framework, the improved model displaced the original RestNet101 feature extraction backbone network by the EfficientNetB4 network for accurate extraction of varied types of WN elements (nodes, arcs, and polygons) in three typical sub-basins in Erhai Lake Basin in 2001, 2008, 2015, and 2023, hence to unveil the spatiotemporal evolution pattern and trend of WN elements across the basin. The study will provide a theoretical basis for ecological governance in Erhai Lake Basin.

Materials and methods

Overview of the study area

The Erhai Lake Basin, China has a complex network of water systems, with a sum of 117 rivers and streams, the basin has 41 small- and medium-sized reservoirs (including Haixihai Reservoir, Cibi River Reservoir, Sancha River Reservoir), 418 ponds, 76 plots of wetland (Zhang et al., 2023). *Figure 1* provides maps of the study area.

http://www.aloki.hu ● ISSN 1589 1623 (Print) ● ISSN1785 0037 (Online)
DOI: http://dx.doi.org/10.15666/aeer/2401_15391561

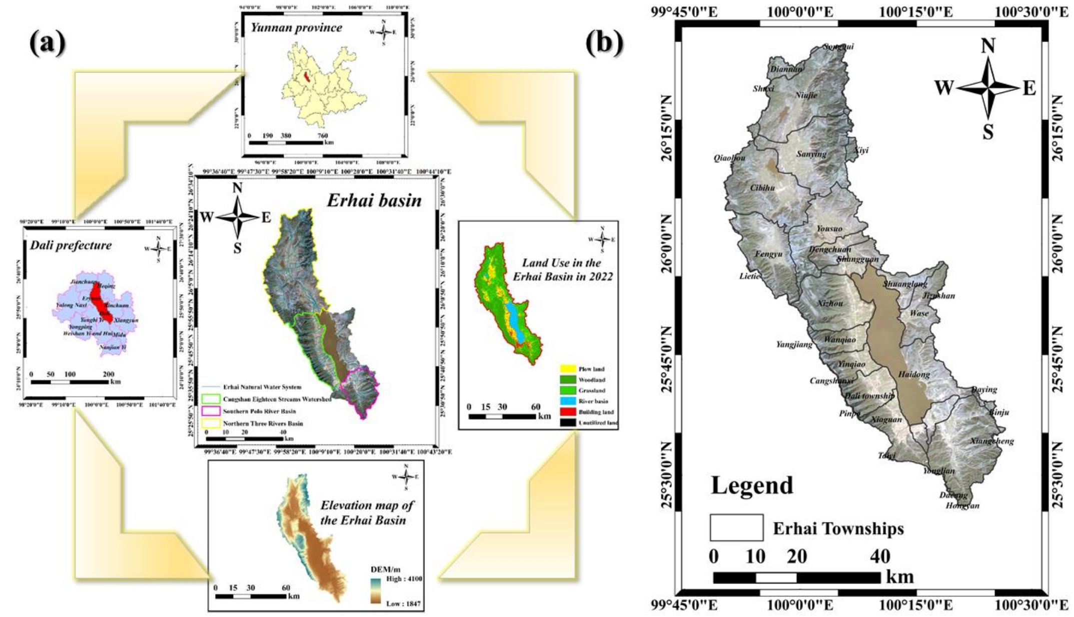

Figure 1. *Maps of the study area (a) Overview of Erhai Lake Basin, (b) Layout of villages and towns in the basin*

In this study, Erhai Lake Basin is divided into three typical sub-basins by soil, land cover, climate, land use, and the water-system structure—Northern Three-River Sub-basin, Cangshan Mountain Sub-basin, and Southern Boluo River Sub-basin, which can be geomorphologically classified into intermountain watersheds, hilly slopes, and mountainous towns, respectively. *Table 1* displays the specifics of the three sub-basins.

Table 1. *Specifics of typical sub-basins in Erhai Lake Basin*

Name	Area (km2)	Annual runoff (million m3)	Percentage in the total inflow to Erhai Lake (%)	Origin	Data sources
Northern Three-River Sub-basin	1389.4	2.45	48.9	Haixihai, Cibi Lake	based on the “One Lake, One Policy” Protection and Governance Action Plan for Erhai Lake (2021–2025) and local hydrological records, from which the values were calculated.
Cangshan Mountain Sub-basin	357.1	1.54	30.7	Cangshan Mountain	
Southern Boluo River Sub-basin	291.3	0.37	17.5	Sanshao Reservoir	
Total	2037.8	4.36	87		

The land use pattern in Erhai Lake Basin exhibits strong spatial heterogeneity: the basin and valley areas are dominated by agricultural land, with rice, corn, and vegetables as the main crops; areas of high and medium altitudes and slopes are dominated by forest land and grasslands, serving ecological functions for water retention and soil protection (Qin and Chen, 2023). Urban and tourist built-up lands stretch along the main roads and the lakeshore, continuing to encroach on farmlands and ecological lands; water bodies and wetlands are scattered across the basin, serving functions of ecological regulation and hydrologic regulation (Li et al., 2022).

http://www.aloki.hu ● ISSN 1589 1623 (Print) ● ISSN1785 0037 (Online)
DOI: http://dx.doi.org/10.15666/aeer/2401_15391561

Data sources and preprocessing

Per fieldwork results, the WN elements in Erhai Lake Basin were divided into three categories—nodes, arcs, and polygons. Nodes include the intersections between water channels and wetlands, between water channels, and between water channels and natural waterways, sluice gates, dams, and culverts, etc.; arcs refer to natural waterways, water channels, and ditches, etc.; polygons include reservoirs, ponds, wetlands, etc.

In this study, the WN data for 2001 and 2008 were Landsat 7 imagery, and those for 2015 and 2023 were Landsat 8 imagery. On 30 October 2023, the research team carried out fieldwork in the Erhai Lake Basin, China. Typical survey sites were arranged along the main inflow rivers, water channels and the lakeshore zone. At each site, a handheld GPS was used to record the spatial locations of key WN nodes, including the intersections between water channels and wetlands, between water channels and natural waterways, and between water channels, as well as sluice gates, dams and culverts. At the same time, cameras and other imaging devices were used to acquire field photographs of water bodies and surrounding land use at each survey site, in order to assist the interpretation of remote-sensing imagery and the verification of WN element types. In addition, we collected information on the location, connectivity and surrounding environment of WN elements in the three typical sub-basins, generated deep-learning semantic segmentation labels (i.e., training sample annotations), and identified suspicious regions that showed discrepancies between the imagery and the actual WN elements. Jilin-1 KF01, GF02, and GF03 Satellite images were used to check and verify the suspicious regions in the primary data for the four years (data sources are presented in *Table 2*). A range of measures were taken to suppress the noises from building shades and vegetation occlusions, and increase the extraction accuracy of water bodies (narrow and meandering rivers, lake boundaries, and fine-grained water bodies): First, radiometric calibration, atmospheric correction, and image fusion were performed on Jilin-1 KF01, GF02, and GF03 images; Second, to improve the model's generalization capacity, the original images and labels were cropped to generate images at a size of 256 × 256; the diversity of the dataset was enriched through data augmentation techinques including flipping, rotation, scaling, translation, and brightness adjustment to prevent the model from overfitting. *Figure 2* shows the technical roadmap of this study.

Table 2. *Sources of data used in this study*

<table>
<tr><th>Type of data</th><th>Source</th><th>Download link</th><th>Resolution</th></tr>
<tr><td>Remote-sensing imagery used for validation in 2022</td><td>JL1GF、JL1KF</td><td>https://www.jl1mall.com/</td><td>0.75m</td></tr>
<tr><td>Remote sensing images of Erhai Lake Basin in 2001 and 2008</td><td>Landsat 7, field surveys</td><td rowspan="2">https://www.gscloud.cn/</td><td rowspan="2">30m</td></tr>
<tr><td>Remote sensing images of Erhai Lake Basin in 2015 and 2023</td><td>Landsat 8, field surveys</td></tr>
<tr><td>Data of DEM, elevation, and slope</td><td>GDEMV2</td><td>http: //srtm.csi.cgiar.org</td><td>30m</td></tr>
<tr><td>Data on natural water systems, natural wetlands, lakes, and roads</td><td>Data Center for Resources and Environmental Sciences (RESDC), China Academy of Sciences</td><td>https://www.resdc.cn/</td><td></td></tr>
</table>

http://www.aloki.hu ● ISSN 1589 1623 (Print) ● ISSN1785 0037 (Online)
DOI: http://dx.doi.org/10.15666/aeer/2401_15391561

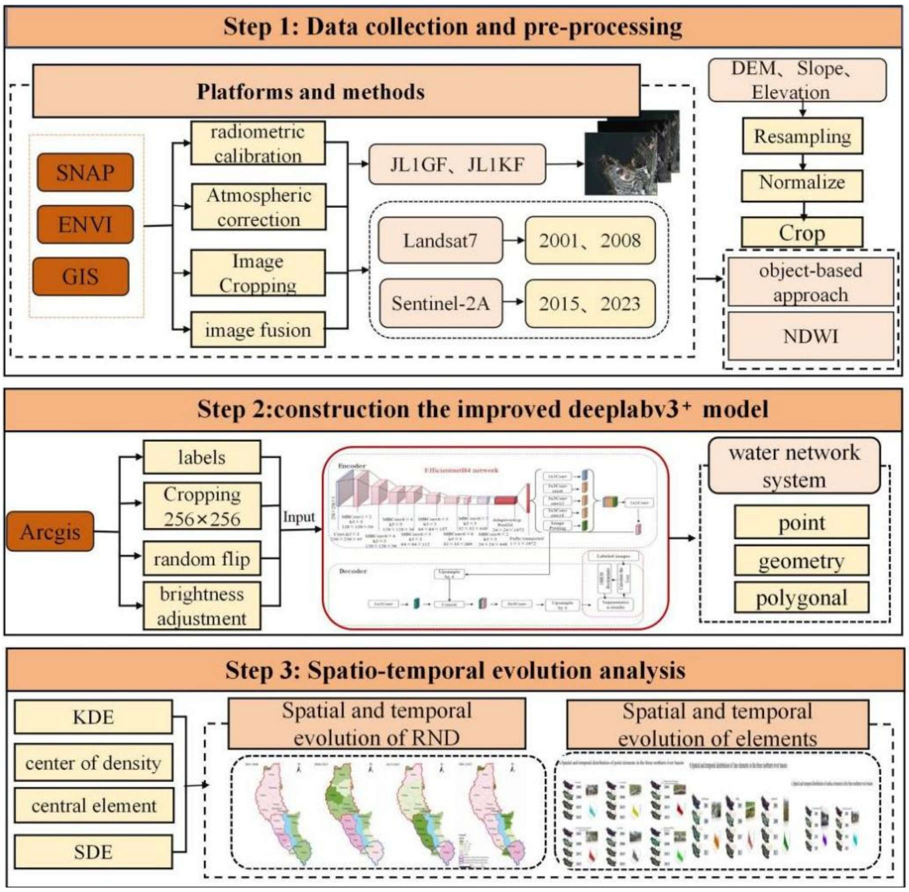

Figure 2. *Technical framework of the study*

Research methods

Improved DeepLabV3$^+$ model

The DeepLabV3$^+$ model was improved as follows: the backbone network of the original DeepLabV3$^+$ model has massive parameters, which will lower the model's feature extraction capacity. In this study, the feature extraction network ResNet101 in the original model was displaced by EfficientNet-B4, which improved the model's efficiency and accuracy through compound scaling, reducing the risks of exploding or vanishing gradients (Tan and Le, 2019); the binary cross entropy (BCE) Loss (Shen et al., 2023) function and Dice Loss (Milletari et al., 2016) were combined and introduced as the joint loss function: the BCE Loss function could perform fine classification at the pixel level, and Dice Loss could address the overlapping of water bodies, making up for the weakness of BCE Loss in processing unbalanced data (Tuo et al., 2025).

Figure 3 shows the architecture of our improved DeepLabV3+ model. The encoder consists of a backbone network and an atrous spatial pyramid pooling (ASPP) module. In the encoder part, the pre-trained EfficientNet-B4 was introduced as the backbone network to extract multi-layer features from the input images. These input images (256 × 256 × 3), after feature extraction and compression through 3 × 3 convolutional layers and multiple MBConv, showed increased channels, and hence 1792-dimensional feature vectors were generated. Multi-scale atrous convolution was then implemented on these feature vectors to extract multi-scale features and generate deep feature maps with rich

http://www.aloki.hu ● ISSN 1589 1623 (Print) ● ISSN1785 0037 (Online)
DOI: http://dx.doi.org/10.15666/aeer/2401_15391561

contextual information. In the decoder part, the model performed 4× upsampling on the feature maps output from the encoder and merged these deep-level feature maps with lower-level feature maps through feature fusion. The merged feature maps then underwent 3 × 3 convolution to reduce the number of channels and augment key information. Post convolution, 4× upsampling was implemented to recover the resolution of the feature maps to the resolution of the original images. Next, the predictions were compared with the actual labels, the loss was calculated, and the model's parameters were updated through backpropagation. Last, the model output the segmentation results of the same size as the original images.

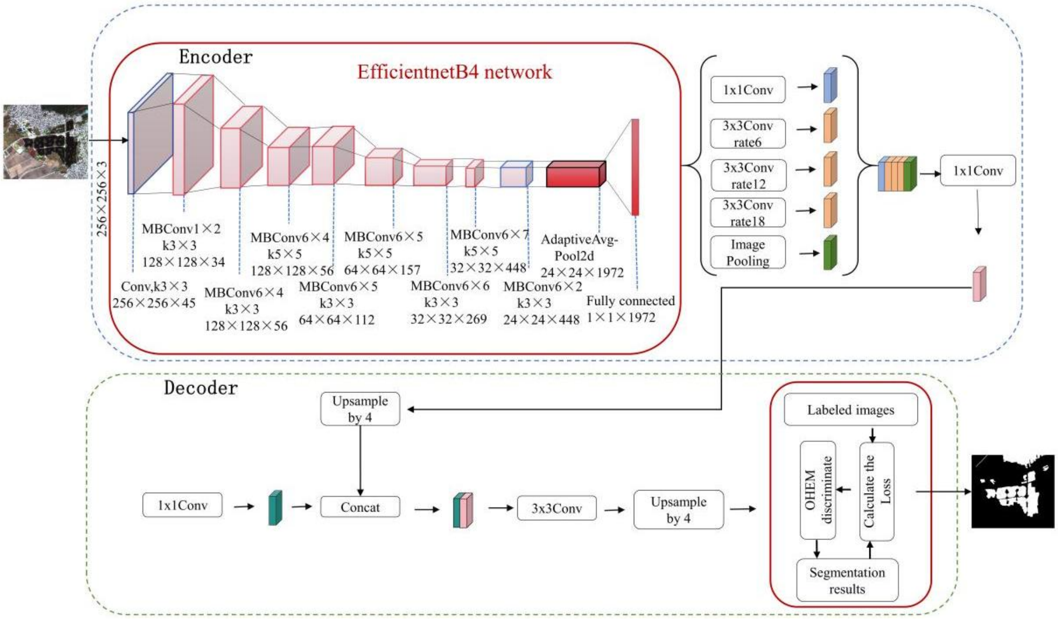

Figure 3. *Architecture of the improved DeepLabV3$^+$ model. Note: The parts enclosed in red boxes represent the improved modules of the model, while the remaining parts correspond to the original modules*

To verify the accuracy and adaptability of our feature extraction method, we compared the improved DeepLabV3$^+$ model, the normalized difference water index (NDWI) method, and the object-oriented approach to identify the optimal WN element extraction solution and thereby provide the required data for subsequent analysis of WN evolution in the study area. In this study, the NDWI was used as a band-ratio index to separate water from non-water features. Taking advantage of the strong absorption of near-infrared (NIR) radiation by water and the strong reflection of NIR by vegetation, the ratio between the green and NIR bands can effectively suppress vegetation information and enhance surface water signals (McFeeters, 1996; Purnam et al., 2024). The NDWI is defined as:

$$NDWI = \frac{Green - NIR}{Green + NIR} \qquad \text{(Eq.1)}$$

where Green and NIR denote the brightness values of the green and near-infrared bands, respectively, corresponding to bands B2 and B4 of the imagery.

http://www.aloki.hu ● ISSN 1589 1623 (Print) ● ISSN1785 0037 (Online)
DOI: http://dx.doi.org/10.15666/aeer/2401_15391561

Analysis of density, central zone, and non-central zone

Kernel density estimation

Kernel density analysis (KDE) is a non-parametric method for estimating the density distribution of spatial data. By inputting point and arc datasets into the tool, the spatial distribution trends of the water-network (WN) system can be effectively analyzed.The kernel density calculation equation is presented as follows (Mashuri et al., 2021):

$$\widetilde{f(\dot{x})} = \frac{1}{nh}\sum_{i=1}^{n} K(\frac{x-x_i}{h}) \qquad \text{(Eq.2)}$$

where h is the window width, or the smoothing function, K( ) is the kernel function, n is the number of samples. As can be inferred from the equation, when n is infinitely large and the window width approaches 1, $\widetilde{f(\dot{x})}$ converges in probability to f(x).

Density center, central element

Using the density center, we locate the density centroid of the water-network (WN) system in the three typical sub-basins of the Erhai Lake Basin as shown in *Eq.(3)*:

$$\bar{X} = \frac{\sum_{i=1}^{n} x_i}{n}, \quad \bar{Y} = \frac{\sum_{i=1}^{n} Y_i}{n} \qquad \text{(Eq.3)}$$

where x_i and Y_i is the coordinates of the element i, and n is the sum of elements. To obtain the weighted average of the density center, we can extend the equation to *Eq. (4)*:

$$\bar{X}_w = \frac{\sum_{i=1}^{n} x_i w_i}{w_i}, \quad \bar{Y}_w = \frac{\sum_{i=1}^{n} Y_i w_i}{w_i} \qquad \text{(Eq.4)}$$

where wi is the weight of the element i.

By calculating, for each element, the minimum cumulative distance to the centroids of the other elements, we identify the central element of the WN system in each sub-basin. The specific equation is shown in *Eq. (5)*:

$$X = \frac{\sum_{i=1}^{n} x_i C_i}{\sum_{i=1}^{n} C_i}, \quad Y = \frac{\sum_{i=1}^{n} Y_i C_i}{\sum_{i=1}^{n} C_i} \qquad \text{(Eq.5)}$$

where X, Y specify the coordinates of the central point; x_i and Y_i are the coordinates of the ith element, and Ci is the number of the elements i.

To identify the central and non-central zones of the WN system, WN density was first calculated for each year at a 30 m × 30 m grid resolution over the entire sub-basin, and the density values were classified into five levels using the natural breaks (Jenks) method. Contiguous patches composed of cells in the highest density class were merged and defined as the WN “central zone”, while the remaining density classes were grouped as the “non-central zone”. On this basis, the area and centroid coordinates of the central zone were calculated for each period, and the spatial migration of the central zone was analysed over time.

http://www.aloki.hu ● ISSN 1589 1623 (Print) ● ISSN1785 0037 (Online)
DOI: http://dx.doi.org/10.15666/aeer/2401_15391561

Directional distribution (standard deviational ellipse)

The standard deviational ellipse (SDE) characterizes geographic distribution trends by the dispersion and orientation of observed samples. It summarizes the spatial characteristics of geographic features—central tendency, dispersion (spread), and directional trend. The ellipse's attribute values include the X and Y coordinates of the mean center, two standard distances (major and minor axes), and the orientation (azimuth) of the ellipse.as shown in *Eq. (6)* (Zhao et al., 2022):

$$U = \begin{pmatrix} Var(x) & Cov(x,y) \\ Cov(y,x) & Var(y) \end{pmatrix} = \frac{1}{n}\begin{pmatrix} \sum_{i=1}^{n} x'^{2}_{i} & \sum_{i=1}^{n} x'_i y'_i \\ \sum_{i=1}^{n} x'_i y'_i & \sum_{i=1}^{n} y'^{2}_{i} \end{pmatrix} \quad \text{(Eq.6)}$$

where x and y specify the coordinates of the element i, $\bar{x}$ and $\bar{y}$ are the coordinates of the mean center, $\mathrm{Var}(x)$ and $\mathrm{Var}(Y)$ are the variance of x and y, respectively, and $\mathrm{Cov}(x, y)$ is the covariance of x and y.

Results and analysis

Extraction of WN elements in typical sub-basins

Extraction of WN elements in Northern Three-River Sub-basin

As shown in the Jilin-1 Satellite remote-sensing imagery, in the Northern Three-River Sub-basin exhibited a high density of WN elements; the three main rivers there—Miju River, Luoshi River, and Yong'an River—flow southwards and branch into several tributaries. These tributaries and the main streams shape a regularly distributed dendritic pattern and form a complex WN structure in the sub-basin.

As *Figure 4* shows, all three methods could accurately extract the polygon elements in the Three-River Sub-basin in the north, and the extractions were visually identifiable. However, discontinuities were observed in the extractions by NDWI and object-oriented methods. For instance, in the zoomed-in images of area b1 in *Figure 4*, the improved DeepLabV3$^+$ model showed strong performance in segmenting fine-grained water bodies, and identified the claw-like dendritic pattern of the WN of the three main rivers that join Erhai Lake—Miju River, Luoshi River, and Yong'an River, which best preserved the continuity of rivers in the extraction process. NDWI performed poorly in extracting fine-grained water bodies, and its extracted polygon elements showed vague boundaries. As the extraction results of c1 in *Figure 4* show, NDWI barely detected pixels of fine-grained water bodies and exhibited substantial noise, resulting in a high rate of missed extraction. The extraction of the area d1 in *Figure 4* shows that the object-oriented technique resolved the shortcoming of NDWI, but it exhibited fragmented drainage patterns and misclassified the pixels of areas under the shades of mountains.

Extraction of WN elements in Cangshan Mountain Sub-basin

According to the Jilin-1 Satellite imagery, the WN in Cangshan Mountain Sub-basin exhibited a radial pattern and had relatively homogenous elements; originating from Cangshan Mountain, the water flows in the sub-basin converge in regions along the main watershed divides of the mountain, where the tributaries are interwoven with the main streams, giving shape to a densely interconnected water network.

http://www.aloki.hu ● ISSN 1589 1623 (Print) ● ISSN1785 0037 (Online)
DOI: http://dx.doi.org/10.15666/aeer/2401_15391561

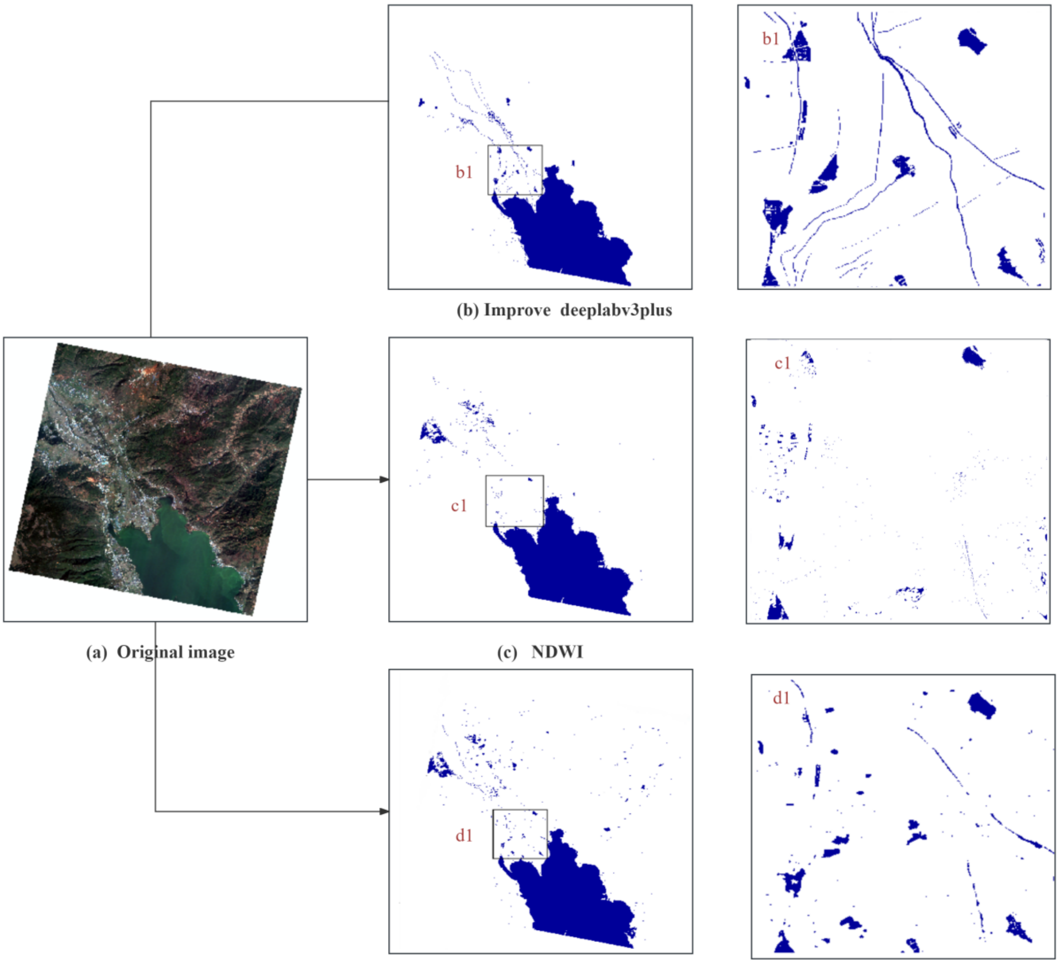

Figure 4. *Extraction of WN elements in Northern Three-River Sub-basin. Note: Blue areas indicate the extracted water-network (WN); white denotes the background; black boxes mark the key comparison regions*

As the zoomed-in image of the area b1 in *Figure 5* shows, the improved DeepLabV3+ model showed excellent performance in extracting arcs, and well identified the contours of natural waterways and Erhai Lake; However, discontinuities remained in the extraction of fine-grained water bodies and some tributaries due to limitations in resolution or modelling capacity. Overall, our improved model showed good performance in WN element extraction. The NDWI method misclassified the shades of the Cangshan Mountain as water bodies. As the extraction results of the key area c1 to the west of Erhai Lake in *Figure 5* show, the NDWI method failed to accurately extract small rivulets, natural waterways and water channels, showing omissions in extraction. The object-oriented technique alleviated the problem of misclassifying mountain shades as water bodies, but its performance in extracting main rivers was unsatisfactory: as the zoomed-in image of the area d1 in *Figure 5* shows, it only managed to detect scattered pixels of Yinxian River and Zhonghe River, but could not maintain the spatial continuity of the WN elements.

http://www.aloki.hu ● ISSN 1589 1623 (Print) ● ISSN1785 0037 (Online)
DOI: http://dx.doi.org/10.15666/aeer/2401_15391561

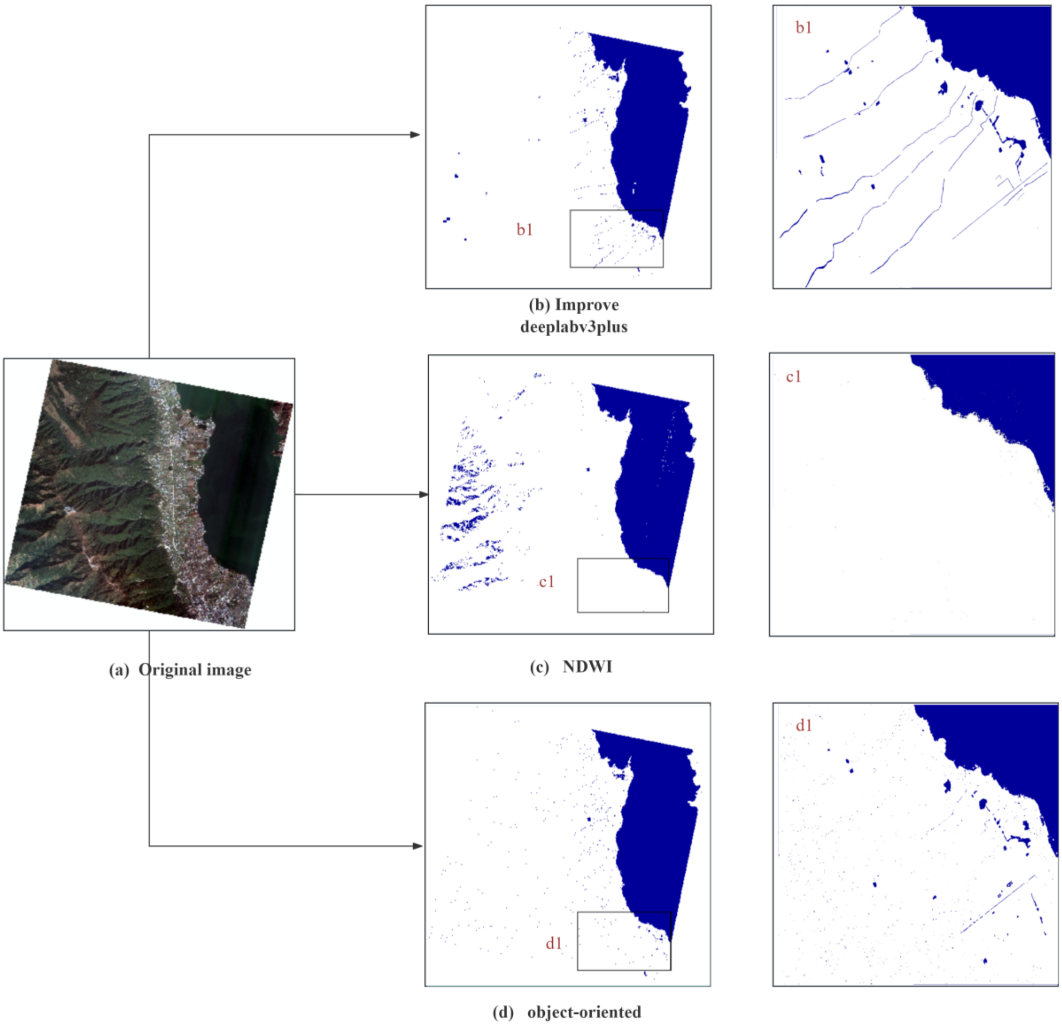

Figure 5. *Extraction of WN elements in Cangshan Mountain Sub-basin*

Extraction of WN elements in Boluo River Sub-basin

The waterways in the Boluo River Sub-basin have irregularly-shaped paths, where the tributaries exhibit substantially different widths and flow volumes, resulting in a typically fragmented drainage network; moreover, the presence of small rivulets, wetlands, and seasonal water bodies leads to a dispersed distribution of WN elements, which accounts for the blurring contours of water bodies in the high-resolution remote-sensing imagery. Therefore, this study took a regional zoomed-in image of the Boluo River Sub-basin to demonstrate the extraction effects of different methods and avoid possible misinterpretations of the global map that might arise from regional heterogeneity.

As *Figure 6* shows, the Boluo River Sub-basin in the south of Erhai Lake Basin exhibits topographical complexity, where the intertwining mountains, hills, and rivers lead to an irregularly-shaped water network there, and the distribution of water flows is largely subjected to regional geographical conditions. The intersections between water channels and natural waterways have complex surroundings, where the spectral information changes due to occlusion from riparian vegetation and buildings, so the NDWI and object-oriented methods suffered the problem of omitted extraction. The

http://www.aloki.hu ● ISSN 1589 1623 (Print) ● ISSN1785 0037 (Online)
DOI: http://dx.doi.org/10.15666/aeer/2401_15391561

improved DeepLabV3+ model, however, maintained the integrity of the arc elements in extraction and did not show misclassification or omissions, demonstrating its strong performance in segmenting small targets.

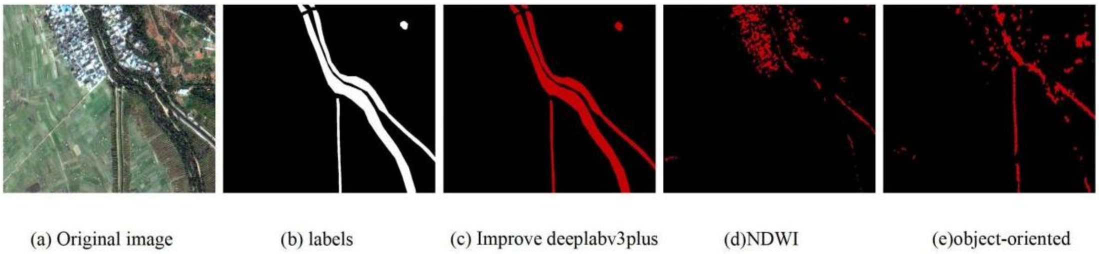

Figure 6. *Extraction of WN elements in Boluo River Sub-basin*

Accuracy comparison

To measure the accuracy of our proposed model, this study took the visual interpretations of the high-resolution remote-sensing imagery as the truth values, and compared the binary extraction results obtained by the three methods with the truth values to generate confusion matrices. The metrics, including precision, recall, F1-score, false extraction rate, and omitted extraction rate, were used to evaluate the extraction accuracy (Qiao et al., 2021; He et al., 2023). *Table 3* shows the comparison and evaluation results.

Table 3. *Extraction accuracy comparison*

Metric	Improved DeepLabV3+	NDWI	Object-based
Precision, %	98.87	94.32	94.80
Recall, %	99.30	93.73	98.90
F1-Score	99.08	96.62	96.8
Commission error, %	1.13	5.68	5.20
Omission error, %	0.70	6.27	1.10

As *Table 3* shows, our improved DeepLabV3+ model reached a precision, recall, and F1-score of 98.87%, 99.30%, and 99.08%, respectively, all higher than the values achieved by the other two traditional methods. Our model reached a false extraction rate of 1.13%, much lower than 5.68% achieved by the NDWI method; the high false extraction rate also resulted in a high omitted extraction rate, making the NDWI method fail to detect actual WN elements. Our model also achieved the smallest omitted extraction rate (0.7%), significantly lower than 1.1% achieved by the object-oriented method and 6.27% by the NDWI method.

In sum, our improved DeepLabV3+ model outperformed the other two traditional approaches: it effectively suppressed the noises caused by shades of buildings and extracted complete WN elements, with outstanding performance in extracting fine-grained water bodies.

http://www.aloki.hu ● ISSN 1589 1623 (Print) ● ISSN1785 0037 (Online)
DOI: http://dx.doi.org/10.15666/aeer/2401_15391561

Spatiotemporal evolution WN elements in typical Sub-basins

Spatiotemporal evolution of WN elements in the Northern Three-River Sub-basin

As *Figure 7* shows, the elements (nodes, arcs, and polygons) Northern Three-River Sub-basin have witnessed extensive spatiotemporal changes over the years. Specifically, in this region, the six node elements were evenly distributed around the farmland and increased with time: from 2001 to 2008, the nodes increased mildly to 1249, where one node element, i.e., intersections between water channels (small water gates), saw the highest increase and grew to 74; from 2008 to 2015, the nodes had the quickest growth (by 1705) among all elements, where the culvert marked the highest increases among all node elements (by 325 in total). From 2001 to 2023， Among all the node elements, the intersections between water channels (small water gates) saw the highest growth over the years of study, followed by culverts, channels and natural waterways, and then sluice gates, while the barrages had the least increase.

Arc elements in this region showed a different pattern of changes. Specifically, from 2001 to 2015, the length of natural water systems dropped by 123 km, which, however, then rose by 36.81 km from 2015 to 2023. The length of artificial water systems has kept increasing: over the 23 years, the length of water channels has risen by 495.45 km, and the number was 124.25 km in the case of pipes.

The situation with the polygon elements was more complex: natural wetlands and lakes dropped by around 4.99 km^2 from 2001 to 2015, but then witnessed a growth of 3.24 km^2 from 2015 to 2023. The changes in artificial wetlands shared a similar pattern: in 2001–2015, the area of artificial wetlands dropped by 1.61 km^2, which then witnessed a growth of 0.73 km^2 in 2015–2023. When measured by the number of polygon elements, there were 13 fewer natural wetlands and lakes in 2023 than in 2001; the number of artificial wetlands and lakes reduced by 32 from 2001 to 2015, but then witnessed a rise of 24 in 2015–2023.

In summary, in the Northern Three-River Sub-basin, the nodes, water channels, and pipes have increased and grown more closely connected, shaping a unique water network; but natural and artificial water systems and wetlands have shrunk.

Spatiotemporal evolution of WN elements in Cangshan Mountain Sub-basin

As displayed in *Figure 8*, the Spatiotemporal evolution of WN elements in this sub-basin stayed at a medium level among all the three sub-basins, and the nodes in this region were fewer than in the other two sub-basins. The nodes in this region have kept increasing since 2001, increasing by 1034 in 2023, The changes in the length of natural waterways in this region presented an N-shaped curve. In the case of artificial water systems, pipes, and water channels increased steadily by 200.14 km over the 23 years, with drain pipes as the main contributor. In 2023, the sub-basin had 604.36 km of water channels and 80.09 km of pipes.

The area of natural wetland and lakes had a year-by-year decline in 2001-2015 by 2.15 km^2, but increased by 0.57 km^2 from 2015 to 2023. The changes in the artificial wetland were less dramatic: from 2001 to 2015, 39 plots of artificial wetland disappeared, totaling an area of 0.85 km^2, but a recovery of 0.29 km^2 was observed from 2015 to 2023.

In summary, the water network elements in the Cangshan Mountain Sub-basin grew increasingly independent from each other over the 23 years: the streams and brooks were shaping into independent sub-catchments, with the intersections between neighboring streams and brooks decreasing.

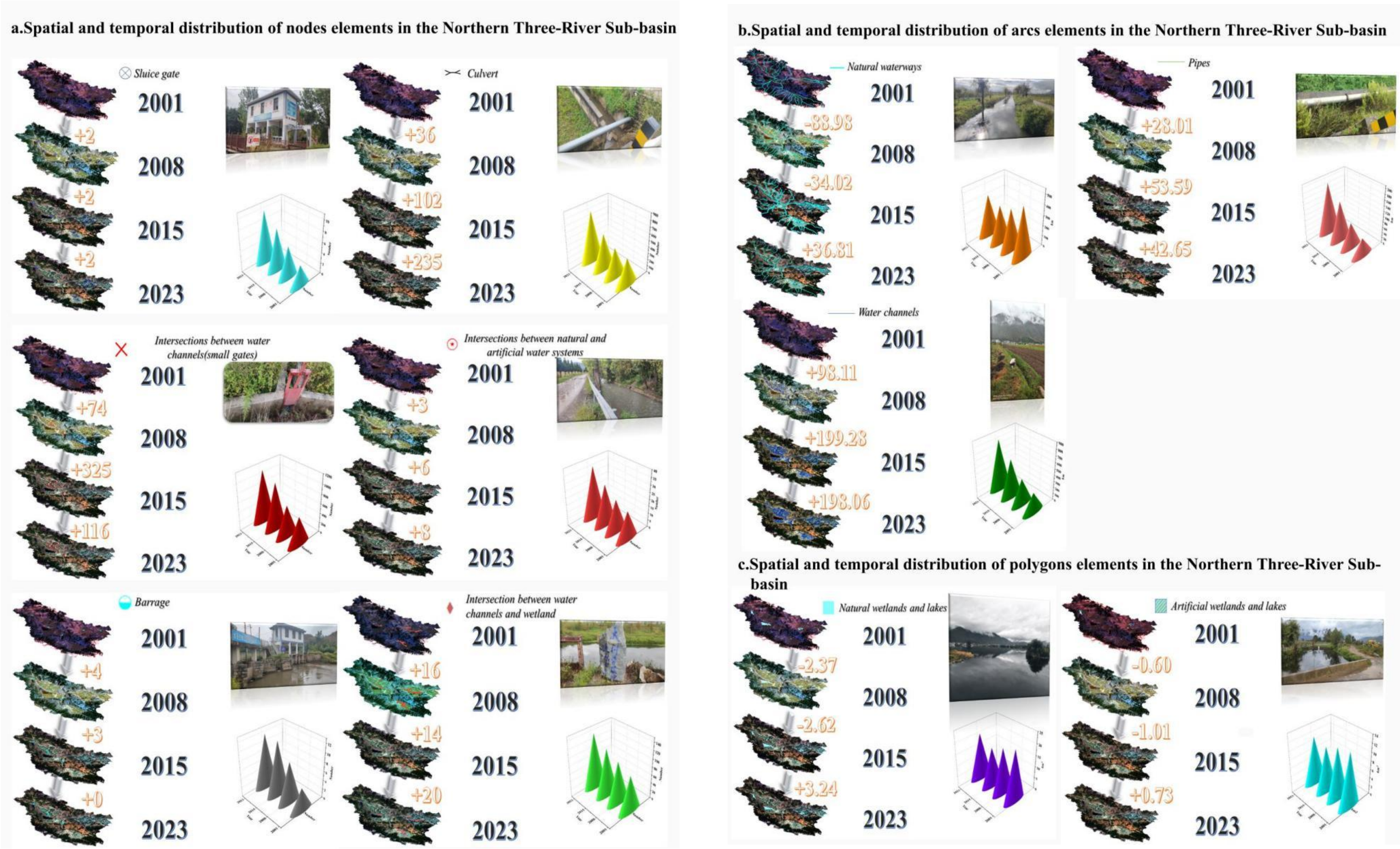

Figure 7. Spatiotemporal evolution of WN elements in the Northern Three-River Sub-basin

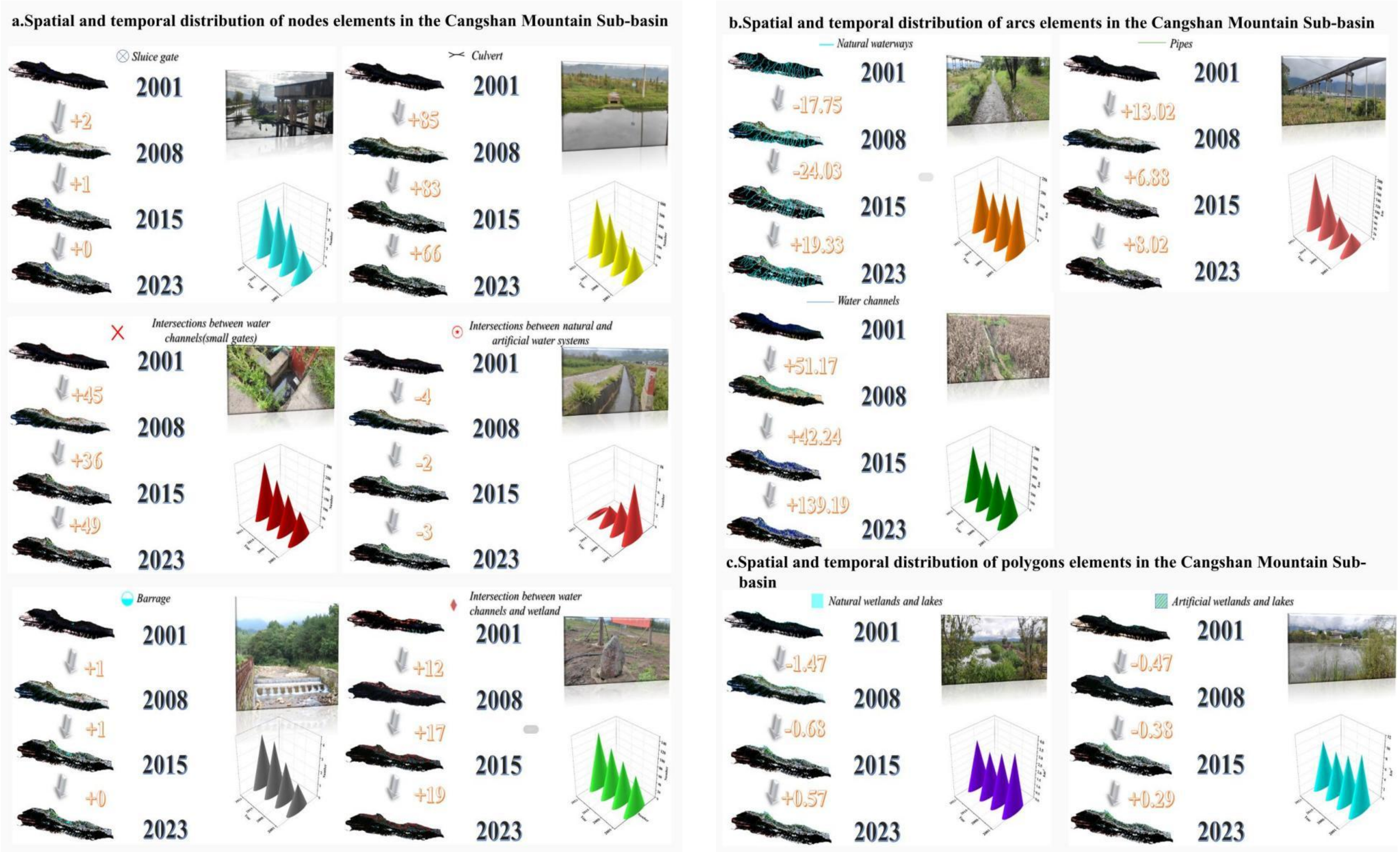

Figure 8. *Spatiotemporal evolution of WN elements in the Cangshan Mountain Sub-basin*

http://www.aloki.hu ● ISSN 1589 1623 (Print) ● ISSN1785 0037 (Online)
DOI: http://dx.doi.org/10.15666/aeer/2401_15391561

Spatiotemporal evolution of WN elements in Boluo River Sub-basin

As *Figure 9* shows, the spatiotemporal evolution in this region were the mildest among all the three sub-basins. Nodes declined from 527 in 2001 to 300 in 2023. Interactions between water channels, culverts, intersections between water channels, and wetlands dropped year by year, but the intersections between water channels and natural waterways and barrages were steadily increasing; while the lengths of water channels and pipes dropped sharply by 8.87 km and 77.83 km, respectively. The changes in natural wetlands and lakes presented a V-shaped pattern: the area dropped by 0.27 km^2 from 2001 to 2015 before seeing a rise of 0.15 km^2 in 2015-2023. The area of artificial wetland, however, has been decreasing over the 23 years, by a total of 0.14 km^2. As far as the number of plots is concerned, the natural wetlands and lakes reduced by 7, and that of artificial wetlands and lakes witnessed a drop of 14.

In sum, as the numbers of nodes, channels, and pipes have increased, the WN in the Northern Three-River Sub-basin has become more complete with tighter connectivity; however, both natural and artificial waterbodies and wetlands have declined in count. In the Cangshan Mountain Sub-basin, WN elements have gradually shifted from interdependence to independence over time, with each stream tending to form its own sub-basin.in the Southern Boluo River Sub-basinin the south, the spatiotemporal evolution has been mild, yet all element types—nodes, arcs, and polygons—exhibit a decreasing trend.To facilitate quantitative comparison, the statistics of WN elements in the three typical sub-basins for 2001 and 2023 are presented in *Table 4*.

Spatiotemporal evolution of WN density in Erhai Lake Basin

As *Figure 10* shows, the WN density in Erhai Lake Basin showed significant variations over the 22 years, with a changing rate within the range of -0.1–0.5 km/km^2. In 2001–2008, the WN density was relatively evenly distributed across the basin, where high densities were mainly observed in Yinqiao Town and Dali Town; medium densities (0.1–0.5) were mainly found in the northern and western parts of the basin (Xizhou Town, Wanqiao Town, etc.), whereas low densities were only observed in a few towns in the eastern and southern parts of the basin (such as Haidong Town and Xiaguan Subdistrict). In 2008–2015, significant changes were observed in the distribution of WN densities in the basin: the area of high-density regions expanded, medium-density regions shrank, while low-density regions significantly increased (such as Niujie Town and Sanying Town); the WN witnessed an overall degradation, showing a pattern of "increased density in the north and declined density in the south". In 2015–2023, the spatial pattern of WN densities experienced further variations: high-density regions shifted southeastwards; large areas of high-density regions started to occur in Fengyi Town and the southern part of the basin, while the regions that used to have a high density, such as Yinqiao Town and Dali Town, experienced a declined WN density. Overall, the WN density exhibited increasing spatial heterogeneity.

In sum, the WN density in Erhai Lake Basin experienced substantial spatiotemporal changes from 2001 to 2023: Spatially, high-density areas shifted from the southwest to the southeast, and the northern part of the basin remained to exhibit a low WN density; temporally, the WN density experienced a shift from a balanced state (2001–2008), to increased spatial heterogeneity and declined density in the northern part (2008–2015), and then to southward migration of high-density area (2015–2023).

http://www.aloki.hu ● ISSN 1589 1623 (Print) ● ISSN1785 0037 (Online)
DOI: http://dx.doi.org/10.15666/aeer/2401_15391561

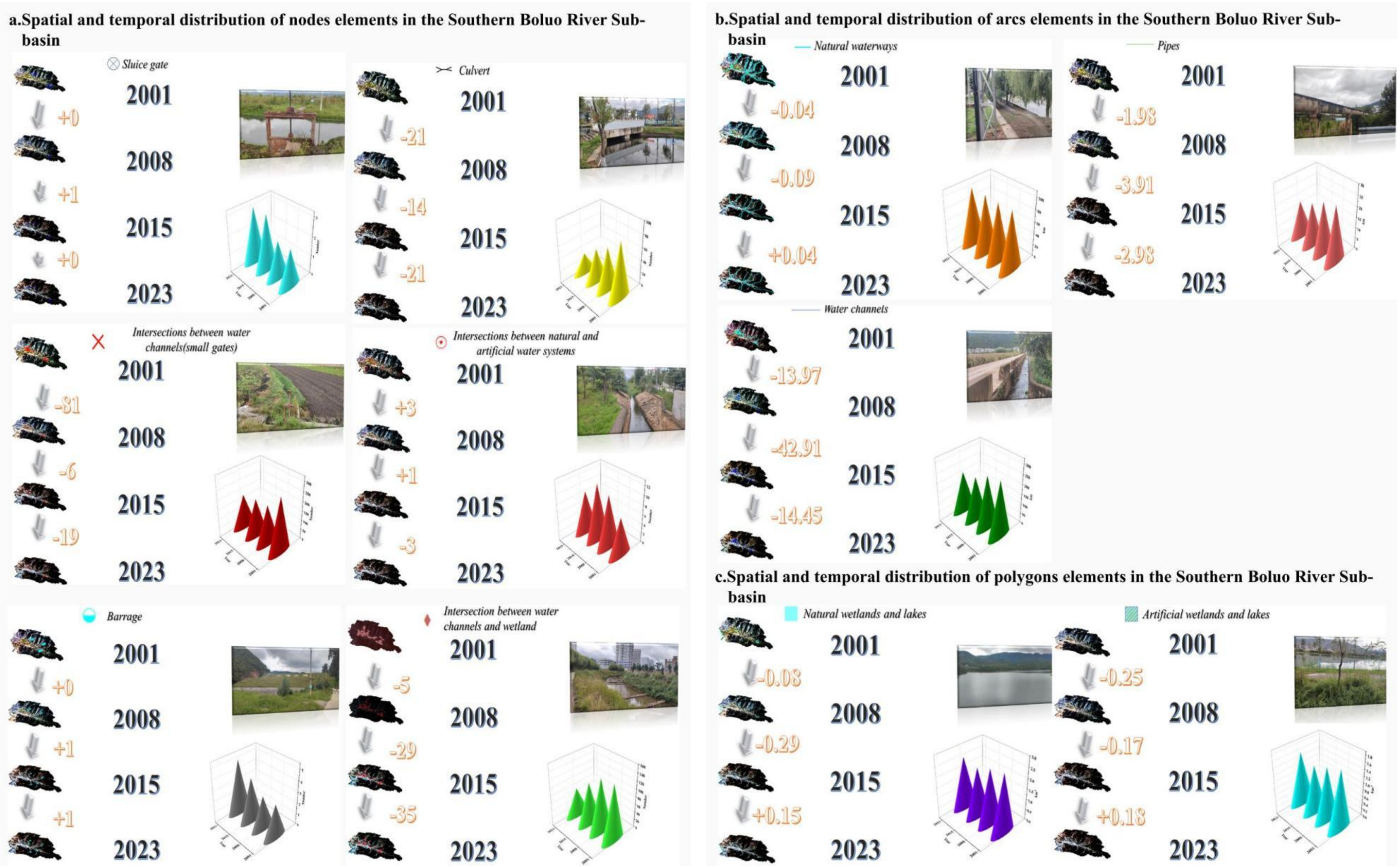

Figure 9. *Spatiotemporal evolution of WN elements in the Southern in Boluo River Sub-basin*

http://www.aloki.hu ● ISSN 1589 1623 (Print) ● ISSN1785 0037 (Online)
DOI: http://dx.doi.org/10.15666/aeer/2401_15391561

Table 4. *Summary of WN elements in the three typical sub-basins in 2001 and 2023*

Sub-basin	Year	Nodes (count)	Arcs (km)	Polygons (km^2)
Northern Three-	2001	946	866.27	34.76
River Sub-basin	2023	2064	1410.25	31.77
Cangshan Mountain	2001	620	709.33	14.64
Sub-basin	2023	1034	887.14	12.50
Southern Boluo	2001	527	404.61	4.51
River Sub-basin	2023	300	324.32	4.11

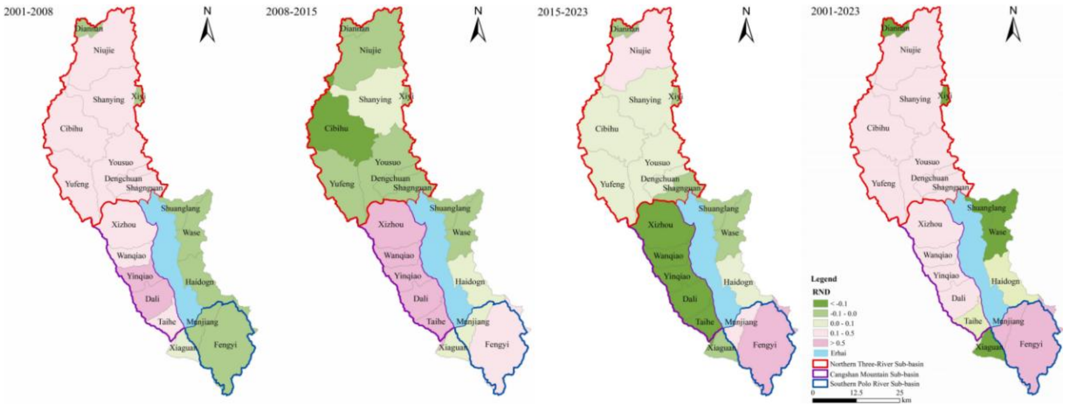

Figure 10. *Spatiotemporal evolution of WN density in Erhai Lake Basin*

Analysis of network density, central zones, and non-central zones

Analysis of Northern Three-River Sub-basin

As *Figure 11* shows, in 2001 and 2008, the density center of this region was closely connected with the central element, both of which were in Sanying Town. In 2015 and 2023, the density center moved to the south of the central element, with a distance of 6.19 km in between. Over these 23 years, the central element moved approximately 2.34 km northwestward, and no substantial changes were observed in the density center.

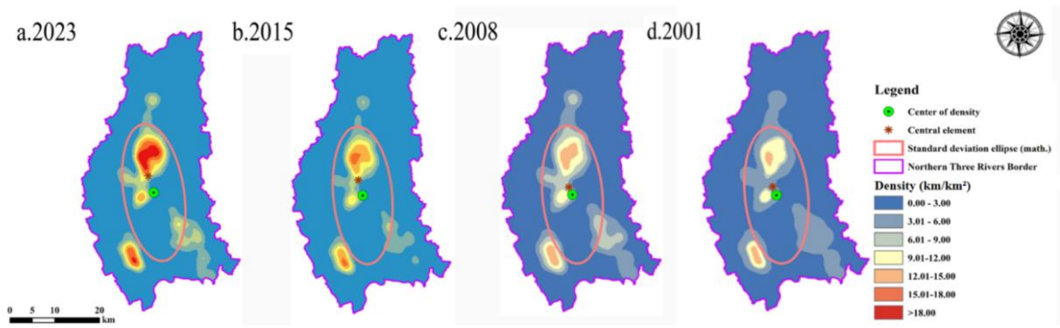

Figure 11. *Density, centrality, and non-centrality of WN elements in Northern Three-River Sub-basin*

In 2001–2023, the directional tilt angle of the standard deviation ellipse turned from 174° to 168°, and the ellipsoid deviated northwestward, but the area of the ellipsoid showed little change (from 325.17 km^2 in 2001 to 326.73 km^2 in 2023), indicating that

http://www.aloki.hu ● ISSN 1589 1623 (Print) ● ISSN1785 0037 (Online)
DOI: http://dx.doi.org/10.15666/aeer/2401_15391561

the central zone changed substantially in this sub-basin, but the area of the central zone showed little variation.

The water network density in this region has been increasing over the 23 years, and the water network systems were concentrated in Sanying Town and Cibihu Town, where the maximum density of 19.37 was observed, followed by the density in Fengyu Town, while Dengchuan Town and Yousuo Town marked the lowest density.

Analysis of the Cangshan Mountain Sub-basin

As *Figure 12* shows, in 2001–2008 the density center of WN elements in the Cangshan Mountain Sub-basin was relatively dispersed from the central element; during 2015–2023, the density center began to converge toward the central element, with the distance between them narrowing to 2.17 km. In addition, the density center was located to the northeast of the central element, while the central element shifted northwestward over the 23-year period. From 2001 to 2023, the density of the water-network system exhibited a year-by-year increase, primarily concentrated in Xizhou Town, with a maximum density of 15.74. The directional tilt angle of the standard deviation ellipse changed from 164° to 161°, and the ellipse progressively shifted northwestward; its area decreased from 91.65 km^2 in 2001 to 85.17 km^2 in 2023.

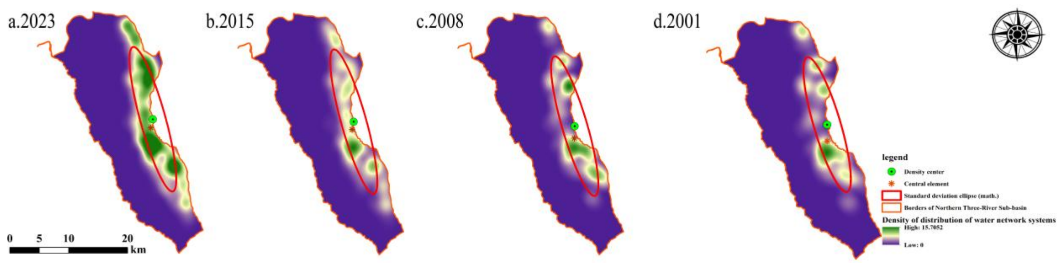

Figure 12. *Density, centrality, and non-centrality of WN elements in Cangshan Mountain Sub-basin*

Analysis of Southern Boluo River Sub-basing

The analysis results of the Southern Boluo River Sub-basin are presented in *Figure 13*. As the figure shows, the density center and central element of this region were closely connected, both of which were in Fengyi Town. In 2001 and 2008, the density center was located to the northwest of the central element; however, it moved to the northeast of the latter in 2015 and 2023. The central element moved eastwards by 1.34 km, while the density center hardly showed any movement.

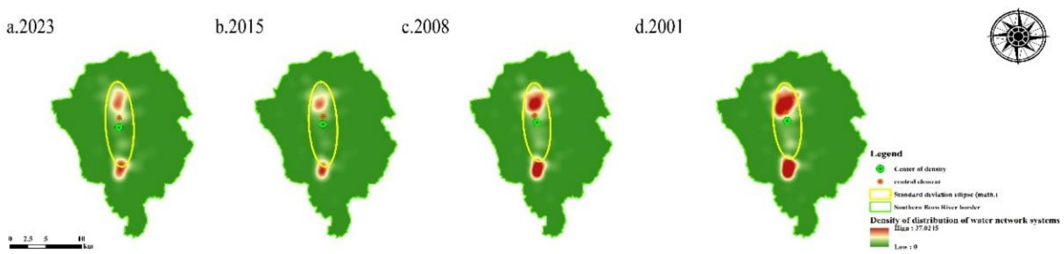

Figure 13. *Density, centrality, and non-centrality of WN elements in Southern Boluo River Sub-basin*

http://www.aloki.hu ● ISSN 1589 1623 (Print) ● ISSN1785 0037 (Online)
DOI: http://dx.doi.org/10.15666/aeer/2401_15391561

Over the 23 years, the tilt angle of the standard deviation ellipse in this sub-basin turned from 176° to 172°, the eccentricity grew steadily, and the area of the ellipsoid increased stably from 31.91km^2 in 2001 to 42.16km^2 in 2023, indicating that the central zone in this watershed has been expanding and moving northeastward since 2001.

In summary, the WN elements density in the Southern Boluo River Sub-basin reduced steadily over the 23 years, with the most drastic drop witnessed in 2008-2015. The WN elements concentrated in Fengyi Town and Sanshao Reservoir, with the density reaching a maximum of 37.03, while the mountainous areas around Fengyi Town marked the lowest density.

Overall, the changes in WN elements differ considerably among the three typical sub-basins of the Erhai Lake Basin, and the statistical results are presented in *Table 5*.

Table 5. *Summary of WN element evolution characteristics in the three typical sub-basins*

Sub-basin	Town with highest WN density	Maximum WN density (km/km²)	Strength of spatiotemporal evolution	Tendency of spatiotemporal evolution	Connectivity
Northern Three-River Sub-basin	Sanying Town	19.37	Strong	Increase	Closely connected
Cangshan Mountain Sub-basin	Xizhou Town	15.70	Moderate	Increase	Independent
Southern Boluo River Sub-basin	Fengyi Town	34.71	Weak	Decline	Moderately connected

Discussion

Multi-factor analysis of WN element extraction

The improved DeepLabV3$^+$ model showed outstanding performance in most regions, but it suffered from discontinuities in the extraction of fine-grained arc elements. This could be attributed to a few factors, such as the river patterns, topographic conditions, solar altitude, and spectral mixture. For instance, the tree canopy shapes and mutual-shading effects would change the reflectance of ground objects, resulting in changes in the spectral features of the boundaries of riverbanks and making extraction more challenging (Luo et al., 2022). Changes in the solar altitude would affect the length and distribution of shadows in the imagery, and a lower solar altitude would project long shadows onto buildings and other ground objects, resulting in spectral confusion. In addition, the issue of mixed pixels is pronounced in high-resolution imagery: the pixels may contain mixed spectral features of both water bodies and surrounding ground objects in regions of narrow streams or rivulets, making classification even more challenging (Alavipanah et al., 2022).

Dynamic degree of water networks in Erhai Lake Basin

It was revealed that strengthened land reclamation and increased water conservancy projects improved the water networks, and this was in line with the findings by Gaucherel et al. (2017). In this study, it was found that the length of natural waterways and the area of wetlands and lakes in the Northern Three-River Sub-basin increased since 2015. The increase could be attributed to the planting area of crops that require high volumes of

http://www.aloki.hu ● ISSN 1589 1623 (Print) ● ISSN1785 0037 (Online)
DOI: http://dx.doi.org/10.15666/aeer/2401_15391561

water and fertilizers, such as garlic and potato, having steadily decreased in the upper reaches of the Basin since 2015, leading to reduced consumption of water by crops (Su et al., 2020). In the Cangshan Mountain Sub-basin, the sub-catchment of each stream had an independent network of water systems; moreover, the water for irrigation and urban greening in this region was directly transferred from Erhai Lake by pipes (Yang et al., 2021). In the Southern Boluo River Sub-basin, there were no tangible changes in the natural waterways and natural wetlands, while the gradual decline in the length of artificial water systems—such as water channels and pipes—could be attributed to the urban expansion of Dali, where the displacement of rural areas by urban land led to a decrease in agricultural infrastructure (Jin et al., 2017; Li et al., 2022).

Differences between the three typical sub-basins in network density, centrality, and non-centrality

There have been considerable differences between the three sub-basins in terms of network density. The northern sub-basin had the lowest density, while the southern sub-basin had the highest density. This difference could be attributed to the area of land the sub-basins take up: the northern watershed has a larger area than the southern one (Zhao et al., 2023b).

In the Northern Three-River Sub-basin, Yousuo Town has a rich network of natural waterways and is home to plenty of natural lakes and wetlands, but the network density there remained low. The cause might be that the town is dominated by built-up land and has a small proportion of farmland, and the artificial water systems are few (Li et al., 2023). The intensive growth in the density of water networks in the northern sub-basin and Cangshan Mountain Sub-basin from 2015 to 2023 could be attributed to the series of governmental initiatives to protect the local environment: in 2015, the government of Eryuan started a range of plans, including “The Six Grand Projects”, “The Seven Grand Movements”, and “The Eight Battles”, to improve the environment in the basin, as well as policies to recover farmland, artificial and natural wetlands (Dong et al., 2022).

Shortcomings and prospect

This study explored the spatiotemporal evolution of water networks in the three typical sub-basins in Erhai Lake Basin. However, the study only coarsely extracted 11 elements in three categories: nodes, arcs, and polygons, from the water networks. The elements can be further divided. For instance, the water channels can be further divided into 1.0 m × 1.5 m channels and 0.7 m × 1.0m channels, or different channels by the construction materials. A finer division of the elements can be performed in future studies on water networks.

The distribution pattern of water networks is subject to a range of factors: construction of large water conservancy projects (Wang et al., 2021), natural and socio-economic influences (Zhai et al., 2025), the game between village administrations (Becker and Easter, 1992), and beyond. However, the contributing factors to the distribution pattern of water networks in Erhai Lake Basin were not investigated in depth in the present work, and more attention should be paid to the response mechanism of water networks to the contributing factors in the basin.

http://www.aloki.hu ● ISSN 1589 1623 (Print) ● ISSN1785 0037 (Online)
DOI: http://dx.doi.org/10.15666/aeer/2401_15391561

Conclusions

This study divided the Erhai Lake Basin into three typical sub-basins, and employed a deep learning semantic segmentation method—the improved DeepLabV3$^+$—to extract WN elements, including nodes, arcs, and polygons, in these three sub-basins in 2001, 2008, 2015, and 2023 to identify the spatiotemporal evolution pattern and trend of the WN elements there. The following conclusions were hence reached:

(1) In this study, an improved DeepLabV3$^+$ model framework was developed to finely extract point, linear and areal WN elements in the Erhai Lake Basin under complex land-cover conditions. Compared with traditional NDWI and object-based methods, it exhibits clear advantages in recognising small water bodies and suppressing interference, providing a transferable technical route for automated detailed mapping and dynamic monitoring in regions with dense water networks.

(2) The evolution characteristics of WN elements show pronounced spatial differences among the three typical sub-basins, reflecting the differential responses of different areas to climate and human activities under the combined effects of urban expansion, water conservancy projects and ecological protection policies. This provides a spatial basis for formulating zoning strategies for inflow-river regulation, restoration of river–lake connectivity and control of agricultural non-point source pollution.

(3) Over the past 22 years, WN density has increased year by year in the Northern Three-River Sub-basin and the Cangshan Mountain Sub-basin, while it has decreased in the Southern Boluo River Sub-basin. The spatiotemporal migration of WN density and its centres reveals that the WN pattern in the Erhai Lake Basin is being reorganised around key towns. Areas with high and strongly varying WN density play multiple roles in irrigation, drainage and pollutant convergence, and should be regarded as priority zones for channel regulation, ecological restoration and water-environment management, whereas areas with low and weakening WN density and connectivity require measures to prevent degradation of ecological functions.

The technical framework and insights of this study can provide decision support for river-network protection, land-use optimisation and integrated watershed management in the Erhai Lake Basin and other plateau-lake basins.

Acknowledgements. This study was supported by the National Natural Science Foundation of China (Grant No. 42361043) and the Scientific Research Fund of the Yunnan Provincial Department of Education (Grant No. 2025Y0528).

REFERENCES

[1] Abed-Elmdoust, A., Miri, M., Singh, A. (2016): Reorganization of river networks under changing spatiotemporal precipitation patterns: An optimal channel network approach. – Water Resour. Res. 52(11): 8845-8860. https://doi.org/10.1002/2015WR018391.

[2] Alavipanah, S. K., Karimi Firozjaei, M., Sedighi, A., Fathololoumi, S., Zare Naghadehi, S., Saleh, S., Naghdizadegan, M., Gomeh, Z., Arsanjani, J. J., Makki, M. (2022): The shadow effect on surface biophysical variables derived from remote sensing: A review. – Land 11: 2025. https://doi.org/10.3390/land11112025.

[3] Becker, N., Easter, K. W. (1992): Dynamic supply from common property resource: Water diversions from the Great Lakes. – Nat. Resour. Model. 6(4): 343-371. https://doi.org/10.1111/j.1939-7445.1992.tb00284.x.

[4] Dong, Y., Guo, Y., Wang, Y., Zeng, W. (2022): Spatial and temporal evolution of the "source–sink" risk pattern of NPS pollution in the upper reaches of Erhai Lake Basin under

http://www.aloki.hu ● ISSN 1589 1623 (Print) ● ISSN1785 0037 (Online)
DOI: http://dx.doi.org/10.15666/aeer/2401_15391561

land use changes in 2005–2020. – Water, Air, Soil Pollut. 233: 202. https://doi.org/10.1007/s11270-022-05662-1.
[5] Feng, Y., Wu, F., Zhang, F. (2024): Environmental statecraft and changing spatial politics: Erhai Lake protection in China. – Polit. Geogr. 115: 103196. https://doi.org/10.1016/j.polgeo.2024.103196.
[6] Gaucherel, C., Frelat, R., Salomon, L., Rouy, B., Pandey, N., Cudennec, C. (2017): Regional watershed characterization and classification with river network analyses. – Earth Surf. Processes Landforms 42(13): 2068-2081. https://doi.org/10.1002/esp.4172.
[7] He, T., Guo, J., Xiao, W., Xu, S., Chen, H. (2023): A novel method for identification of disturbance from surface coal mining using all available Landsat data in the GEE platform. – ISPRS J. Photogramm. Remote Sens. 205: 17-33. https://doi.org/10.1016/j.isprsjprs.2023.09.026.
[8] Jin, G., Deng, X., Yuan, Y., Ma, S., Li, Z., Shi, S. (2017): Scenario simulation of land exploitation and risk assessment of soil erosion in the low-slope hilly area of the Erhai basin. – Phys. Chem. Earth. 101: 78-85. https://doi.org/10.1016/j.pce.2017.01.020.
[9] Kumar, V., Kaushal, R. K., Taloor, A. K., Jain, V. (2021): Incorporation of slope and rainfall variability in channel network extraction from DEM data at basin scale. – Geocarto Int. 37(15): 4425-4440. https://doi.org/10.1080/10106049.2021.1886340.
[10] Li, G., He, T., Zhang, M., Wu, C. (2022): Spatiotemporal variations in the eco-health condition of China's long-term stable cultivated land using Google Earth Engine from 2001 to 2019. – Appl. Geogr. 149: 102819. https://doi.org/10.1016/j.apgeog.2022.102819.
[11] Li, X., Yu, Q., Li, B., Wang, H., Zhang, Y., Liu, H., Xie, X. (2023): Long-term deposition records of microplastics in a plateau lake under the influence of multiple natural and anthropogenic factors. – Sci. Total Environ. 856: 159071. https://doi.org/10.1016/j.scitotenv.2022.159071.
[12] Lin, S.-S., Shen, S.-L., Zhou, A., Lyu, H.-M. (2020): Sustainable development and environmental restoration in Lake Erhai, China. – J. Cleaner Prod. 258: 120758. https://doi.org/10.1016/j.jclepro.2020.120758.
[13] Lu, Y., He, T., Yue, W., Li, M., Shan, Z., Zhang, M. (2023): Does cropland threaten urban land use efficiency in the peri-urban area? Evidence from metropolitan areas in China. – Appl. Geogr. 161: 103124. https://doi.org/10.1016/j.apgeog.2023.103124.
[14] Luo, Y., Feng, A., Li, H., Li, D., Wu, X., Liao, J., Zhang, C., Zheng, X., Pu, H. (2022): New deep learning method for efficient extraction of small water from remote sensing images. – PLOS One 17(8): e0272317. https://doi.org/10.1371/journal.pone.0272317.
[15] Mashuri, M., Ahsan, M., Lee, M. H., Prastyo, D. D. (2021): PCA-based Hotelling's T2 chart with fast minimum covariance determinant (FMCD) estimator and kernel density estimation (KDE) for network intrusion detection. – Comput. Ind. Eng. 158: 107447. https://doi.org/10.1016/j.cie.2021.107447.
[16] McFeeters, S. K. (1996): The use of the Normalized Difference Water Index (NDWI) in the delineation of open water features. – Int. J. Remote Sens. 17(7): 1425-1432. https://doi.org/10.1080/01431169608948714.
[17] Milletari, F., Navab, N., Ahmadi, S.-A. (2016): V-net: Fully convolutional neural networks for volumetric medical image segmentation. – Presented at the 2016 Fourth International Conference on 3D Vision (3DV), Ieee, Stanford, CA, USA, pp. 565-571.
[18] Purnam, K. K., Prasad, A. D., Ganasala, P. (2024): Water indices for surface water extraction using geospatial techniques: a brief review. – Sustainable Water Resour. Manage. 10: 70. https://doi.org/10.1007/s40899-024-01035-0.
[19] Qiao, D. Y., Zheng, J. H., Lu, H., Deng, L. (2021): Application of water extraction methods from Landsat imagery for different environmental background. – Journal of Geo-information Science 23(4): 710-722. DOI:10.12082/dqxxkx.2021.200312.
[20] Qin, H., Chen, Y. (2023): Spatial non-stationarity of water conservation services and landscape patterns in Erhai Lake Basin, China. – Ecol. Indic. 146: 109894. https://doi.org/10.1016/j.ecolind.2023.109894.

[21] Shen, Q., Zhang, H., Xu, Y., Wang, H., Cheng, K. (2023): Comprehensive survey of loss functions in knowledge graph embedding models. – Comput. Sci. 50: 10.

[22] Su, J., Wang, F., Gao, R., Mi, Z., Chen, J., Gu, S. (2020): Water resources allocation in Erhai irrigated district considering catchment water-cycle health. – In: IOP Conference Series: Earth and Environmental Science. IOP Publishing, p. 012105.

[23] Tan, M., Le, Q. (2019): Efficientnet: Rethinking model scaling for convolutional neural networks. – In: International Conference on Machine Learning. PMLR, pp. 6105-6114.

[24] Tang, S., Peng, Y., Chen, Y., Liu, J., Zhang, P., Zhang, Y., He, T., Li, J. (2025): Snow-resilient mapping reveals three decades of surface water expansion on the Qinghai–Tibet Plateau. – Remote Sens. Appl. Soc. Environ. 40: 101769. https://doi.org/10.1016/j.rsase.2025.101769.

[25] Tuo, W., Zeng, J., Wu, F., Wu, W., Wang, X., Zhao, X. (2025): Landslide detection using multimodal data fusion and an improved Deeplabv3+ model. – Sci. Rep. https://doi.org/10.1038/s41598-025-31208-6.

[26] Wang, S., Ji, H., Li, P., Li, H., Zhan, Y. (2020): Growth diffusion-limited aggregation for basin fractal river network evolution model. – AIP Adv. 10. https://doi.org/10.1063/5.0011624.

[27] Wang, J., Lautz, L. S., Nolte, T. M., Posthuma, L., Koopman, K. R., Leuven, R. S., Hendriks, A. J. (2021): Towards a systematic method for assessing the impact of chemical pollution on ecosystem services of water systems. – J. Environ. Manage. 281: 111873. https://doi.org/10.1016/j.jenvman.2020.111873.

[28] Wang, S., Li, G., Feng, C., Xu, W., Wang, X., Nie, Q., Gao, X., Liu, Q. (2023): River system changes and locust breeding area evolution in the Qin-Jin region of the Yellow River Basin during the Ming and Qing dynasties and their disaster effects. – Sci. Total Environ. 880: 163220. https://doi.org/10.1016/j.scitotenv.2023.163220.

[29] Xu, C., Zhang, X., Zhang, J., Chen, Y., Yami, T. L., Hong, Y. (2021): Estimation of Crop Water Requirement Based on Planting Structure Extraction from Multi-Temporal MODIS EVI. – Water Resour. Manage. 35: 2231-2247. https://doi.org/10.1007/s11269-021-02838-y.

[30] Yan, C., Lu, X., Zhao, X. (2008): Protection and sustainable utilisation of water resources in Lake Erhai basin. – Int. J. Sustainable Dev. World Ecol. 15(4): 357-361.

[31] Yang, L., Xu, Y., Han, L., Song, S., Deng, X., Wang, Y. (2016): River networks system changes and its impact on storage and flood control capacity under rapid urbanization. – Hydrol. Processes 30(13): 2401-2412. https://doi.org/10.1002/hyp.10819.

[32] Yang, F. L., Zhang, X. Z., Li, J. H., Zhao, H. F., Jin, F. M., Zhou, B. X. (2021): Analysis and evaluation of the treatment and reuse of tailwater: A case study in Erhai Lake. – J. Cleaner Prod. 327: 129435. https://doi.org/10.1016/j.jclepro.2021.129435.

[33] Zhai, G., Zhang, M., Hu, Y., Chen, Y., Wu, C., Lu, Y., He, T. (2025): Nighttime light metrics for analysing urban-rural economic disparities: A case study in 36 Chinese metropolitan areas. – Cities 162: 105930. https://doi.org/10.1016/j.cities.2025.105930.

[34] Zhang, Y. B., Chen, Y., Jiang, F., Deng, Z., Xie, Z., Zhang, Y. N., Wen, P. (2023): A comprehensive study of the suitability of urban underground spaces for connection development: A case study of the Erhai lake basin, China. – Sustainability 15(9): 7433. https://doi.org/10.3390/su15097433.

[35] Zhao, Y., Wu, Q., Wei, P., Zhao, H., Zhang, X., Pang, C. (2022): Explore the mitigation mechanism of urban thermal environment by integrating geographic detector and standard deviation ellipse (SDE). – Remote Sens. 14: 3411. https://doi.org/10.3390/rs14143411.

[36] Zhao, H., Li, J., Zheng, H., Li, J. H., Wang, J., Liao, L., Ge, X., Chen, Y., Guo, X., Zeng, W. (2023): Effects of Fertilization of Different Crops on Non-Point Source Pollution in the Upper Reaches of Erhai Lake Basin. – Water, Air, Soil Pollut. 234: 581. https://doi.org/10.1007/s11270-023-06595-z.